Cancer Immunity, Vol. 4, p. 6 (23 July 2004) Submitted: 25 November 2003. Accepted: 29 March 2004.
Communicated by: RD Schreiber

RNA interference of IL-10 in leukemic B-1 cells

Brian A. McCarthy, Amal Mansour, Yi-Chu Lin, Sergei Kotenko, and Elizabeth Raveche

UMDNJ-New Jersey Medical School, Department of Pathology and Laboratory Medicine, Newark, NJ, USA

Keywords: chronic lymphocytic leukemia, B-1 cell line, RNA interference, IL-10, cell cycle, apoptosis

Abstract

RNA interference, or RNAi, is designed to work by Watson-Crick base pairing and to result in a posttranscriptional block in protein synthesis. Antiapoptotic proteins are a major focus of cancer therapy and make attractive targets for RNAi. An IL-10 RNAi sequence was designed in accordance with Tuschl rules and was modeled to a hairpin configuration. In chronic lymphocytic leukemia (CLL), the most common leukemia in the Western world, the failure to undergo apoptosis may be responsible for the accumulation of malignant B-1 cells. Interleukin-10, despite controversy, has been shown to have antiapoptotic properties, and increased endogenous IL-10 production has been found in CLL by several labs. A malignant B-1 cell line, LNC, derived from an NZB mouse (a murine model for CLL) was utilized as a target for IL-10 RNAi. Our earlier studies of antisense IL-10 resulted in antiproliferative and proapoptotic effects. The cytotoxic effects of IL-10 RNAi were dose- and time-dependent, with an optimal dose 10-fold lower than that of antisense IL-10. IL-10 RNAi lowered IL-10 protein as measured by ELISA. 2 µM IL-10 RNAi initiated a G2/M block and a decrease in the message for cdc25C, the M-phase inducer phosphatase. IL-10 RNAi efficiently induced apoptosis. *Bcl7C*, a member of the antiapoptotic *Bcl* family, was significantly down-regulated. IL-10 modulating *Bcl7C* expression represents a novel mechanism in the evasion of apoptosis. This approach, by itself or in conjunction with current therapies, merits consideration in similar B-cell malignancies.

Introduction

Although many metastatic tumors produce IL-10, a potent anti-inflammatory agent, to block the antitumor response, the role of IL-10 in leukemia is still controversial. In an early study, investigators found that the CLL patients they studied did not have detectable IL-10 in their sera, and exogenous IL-10 administration to cultured CLL cells led to apoptosis (1). They did not note this phenomenon in other malignant B-cell samples in their possession. Subsequently, several possible methodological problems for their observations were noted in the literature (2, 3), particularly the use of fresh versus frozen specimens. Other labs have since found IL-10 in B-CLL samples (4, 5). When analyzing 151 CLL patients by ELISA, Fayad *et al*. found serum IL-10 levels were

higher in CLL patients (median 5.04 pg/ml) than in normal volunteers (median undetectable, n = 55). They also found that when analyzed individually or in combination with IL-6, elevated IL-10 was an independent prognostic factor for decreased survival (6). This paper seeks to elucidate the specific genes and pathways involved with IL-10 in leukemia. Elaborating the antiapoptotic mechanisms of IL-10 has implications in the treatment of cancer. In this report the apoptotic-inducing properties of blocking IL-10 are examined in a leukemic cell line.

As a source of malignant B-1 cells, we used an *in vitro* established cell line, LNC (7), derived from the lymph node of an NZB mouse, which is used as a murine model of CLL (8). LNC expresses high levels of IL-10, and following *in vivo* transfer, results in a fatal B-1 malignant expansion. In contrast, NZB *IL-10* (-/-) knockout mice overwhelmingly fail to develop leukemic symptoms (9). The antiproliferative effects of antisense IL-10 on B lymphocytes were reported previously (10), and additionally, an increased requirement for IL-10 was demonstrated during the malignant process (11). Earlier lab work utilizing antisense IL-10 demonstrated a G2/M cell cycle block and apoptosis, whereas Western analysis showed decreased levels of $p27^{Kip1}$ (12). This paper seeks to extend this research with the administration of IL-10 RNAi and the examination of critical cell cycle components and apoptosis regulators.

Previous work showed that double-stranded RNA could inhibit translation (13, 14, 15, 16, 17, 18). This effect has several names, including RNAi and posttranscriptional silencing. RNAi is now a widely used technique that has been used in a variety of systems to decrease target gene expression (19, 20, 21, 22, 23, 24, 25, 26, 27, 28, 29, 30). Early observations that hairpin RNA could naturally produce the RNAi effect led our lab to model the IL-10 RNAi sequence used in this experiment (31, 32, 33). The production of optimum RNAi effects not only depends on biological factors affecting the target, such as RNA folding (34), but on the need to avoid interfering with other, similar, proteins. The idea that the malignant B-cell line, LNC, would take up RNAi free-floating in the media was based on work demonstrating RNAi uptake by simply soaking worms and allowing for ingestion of the RNAi sequence (35).

IL-10 was chosen as a target for RNAi based on its regulatory role in the immune response. IL-10 was initially described as a cytokine synthesis inhibitory factor (36). *IL-10*-deficient mice can develop severe chronic inflammatory bowel disease, most likely due to the absence of the normally suppressive effect of IL-10 on immune inflammatory responses (37, 38). Tumor cells can take advantage of these immunosuppressive features by producing IL-10. IL-10 production by tumor cells was found to interfere with Taxol® (paclitaxel), allowing malignant cells to better survive treatment with a major chemotherapeutic drug (39). In contrast to its immunosuppressive role, IL-10 is also a co-stimulator for the proliferation of B-cell precursors and B cells following their stimulation by anti-IgM (40). Our lab is interested in the effect of IL-10 on a subset of B cells that are CD5+ and B200 dull, termed B-1 cells. The major producer of B-cell-derived IL-10 is the B-1 cell (41). Elevated IL-10 levels have been found in a variety of tumors and were an independent prognosis factor for decreased response to chemotherapy in patients with advanced gastrointestinal malignancies (42). IL-10 has been found to be elevated in CLL patients in microarray analysis (43). In addition, after treatment with Rituximab, a monoclonal antibody directed at CD20, decreased production of IL-10 was reported in B-cell non-Hodgkin's lymphoma. The authors concluded that this inhibition of IL-10 sensitized these cells to apoptosis, which also supports the role of IL-10 as an antiapoptotic protein (44). In the present study, blocking IL-10 message with IL-10 RNAi produced specific cell cycle and apoptotic effects. These data suggest a role for IL-10 in the protection of a malignant B lymphocyte from apoptosis.

Results

Selection of a target on IL-10 for RNAi

The RNAi sequence was modeled on a hairpin loop after utilizing idealized RNA folding analysis of IL-10 (Figure 1A). Double-stranded RNA occurs naturally in hairpin structures. Although the role of tertiary structure is not clear in RNAi, a target sequence that is exposed for RNAi binding in the model may be desirable. A 21-nucleotide sequence targeting an amino acid motif at nucleotide 317 was created. This area appears as a hairpin in the idealized model. RNAi and scrambled sequences were diluted in diethylpyrocarbonate (DEPC) water and annealed in annealing buffer for 1 min at 90°C and 1 hr at 37°C. To ensure that sequences were double stranded, RNAi was stained with ethidium bromide and run on an acrylamide gel (Figure 1B). A band can clearly be seen in the dsRNAi lane, but not in the lane for either single strand.

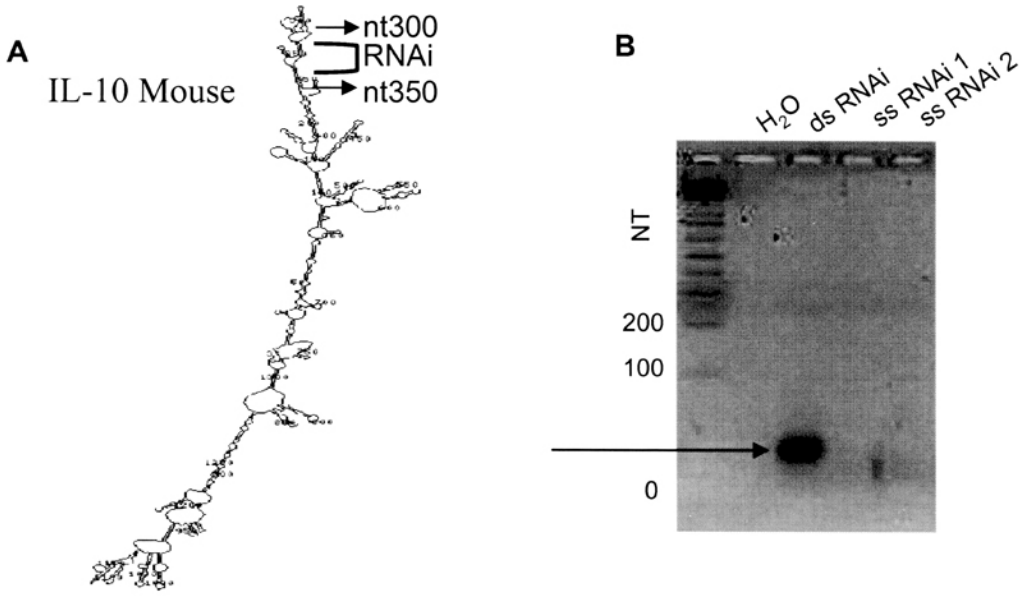

Figure 1. RNAi modeling and annealing. (A) An idealized model of RNA folding for IL-10 based on enthalpy and free-energy calculations. Brackets indicate the location of the mouse IL-10 RNAi employed in these experiments. The sequence begins at nucleotide 317 and appears exposed in a hairpin. (B) Acrylamide gel of RNA stained with ethidium bromide. Lane 1 is dH_2O as a negative control, lane 2 is dsRNAi, lane 3 is ssRNAi strand 1, and lane 4 is ssRNAi strand 2. The size of the ladder on the far left (y-axis) is given in nucleotides. The arrow indicates the band for dsRNAi.

IL-10 RNAi acts in a time-dependent manner

Cellular proliferation of LNC in log growth was measured from an initial concentration of 0.75×10^6 cells per ml (Figure 2). Cells were placed in fresh media before treatment with 2 µM IL-10 RNAi or scrambled IL-10 dsRNA (dsScr). Cells that were untreated or given the scrambled sequences remained in log growth, whereas the RNAi cells stopped proliferating after 24 hr and cell count for the RNAi treatment group was less than the initial concentration at 72 hr.

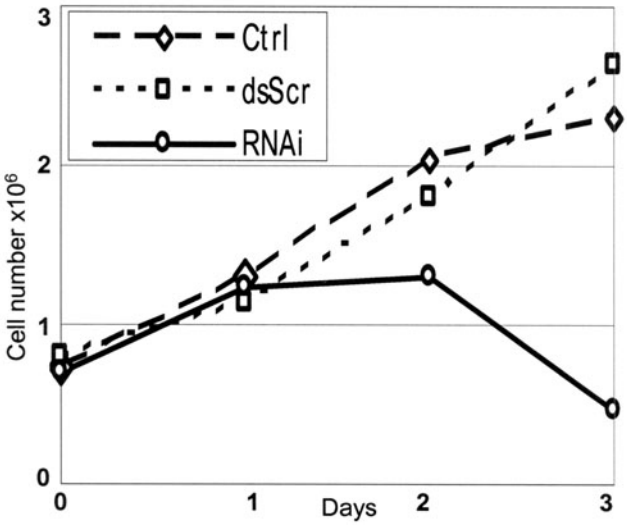

Figure 2. RNAi inhibits cellular growth in a time-dependent manner. The graph shows the cell count over 72 hr of no treatment (dashed line), treatment with 2 µM scrambled IL-10 dsRNA (dsScr, dotted line), and treatment with 2 µM RNAi IL-10 (RNAi, solid line). The x-axis corresponds to the number of days of treatment and the y-axis to the cell number. The graph is representative of triplicate IL-10 RNAi treatments.

IL-10 RNAi acts in a dose-dependent manner

The cell growth response to RNAi was studied by MTT analysis. The MTT assay is a colorimetric assay that quantifies the ability of viable cells to reduce a tetrazolium salt. Dead cells are unable to perform this reduction. Proliferation was examined over the course of 16.5 hr (Figure 3A). Cells in normal log growth were treated with RNAi, with dsScr, or left untreated (control). RNAi inhibited cell growth, whereas the control and dsScr-treated cells experienced normal log growth. MTT analysis demonstrates the decrease in proliferating cells in a dose-related response when compared to untreated or dsScr-treated cells. There was a significant difference between IL-10 RNAi and dsScr in the dose range from 0.5-2 µM ($P < 0.05$). An optimum dose was chosen as 2 µM, and the examination of cell viability was repeated for 48 hr (Figure 3B). Cell viability was decreased by treatment with 2 µM RNAi at 48 hr ($P = 0.0003$).

Cell cycle analysis of IL-10 RNAi treatment

LNC treated with 2 µM IL-10 RNAi exhibited a transient G2/M block at 24 hr with apoptosis at 24 and 42 hr, whereas the scrambled sequences did not (Figure 4). The percentage of apoptotic cells, as measured by PI at 24 hr for RNAi-treated LNC, is 14.33 times that determined for the cells treated with the scrambled sequence (16.05/1.12). After 42 hr of RNAi treatment, the percentage of apoptotic cells cells is 25.77 times that of untreated cells (18.04/.070). Cells were gated to eliminate debris and possibly fragmented cells.

IL-10 RNAi decreases IL-10 protein level as determined by ELISA

IL-10 protein levels in cell supernatants were examined by ELISA after 72 hr of treatment with RNAi or dsScr and were compared to protein levels in untreated cells (Figure 5). RNAi but not dsScr significantly reduced IL-10 protein levels in treated LNC ($P = 0.019$). IL-10 protein was reduced by 64% after RNA interference of IL-10.

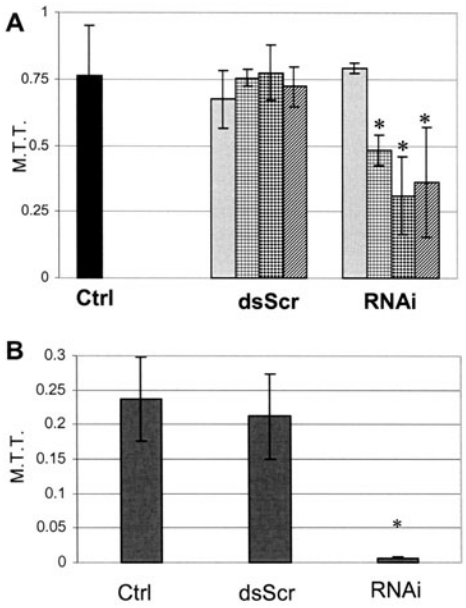

Figure 3. RNAi effectively limits cellular proliferation in a dose-dependent manner. Columns corresponds to treatment groups, with the mean OD values for MTT analysis plotted on the y-axis and the bars corresponding to the standard error of the mean. (A) Cells treated for 16.5 hr with varying concentrations of IL-10 RNAi (RNAi) or scrambled IL-10 dsRNA (dsScr) (0.2-2.0 µM): Gray bar, 0.2 µM ; horizontal stripe, 0.5 µM; diamond bar, 1.0 µM; hatched bar, 2.0 µM. Error bars are the SEM of triplicate results. Asterisks indicate $P < 0.05$ for a Student's *t*-test comparing dsScr to RNAi. (B) Cells treated for 48 hr with 2 µM RNAi or dsScr. Error bars are the SEM of triplicate results. Asterisks indicate $P < 0.05$ for a Student's *t*-test comparing dsScr to RNAi.

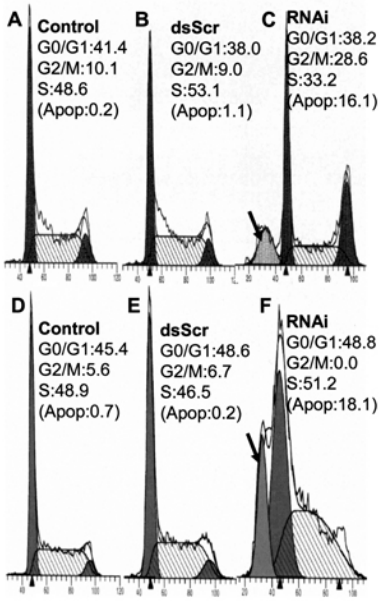

Figure 4. RNAi induces a G2/M block and apoptosis. Histograms showing PI staining of DNA content, with the x-axis reflecting DNA content and the y-axis the cell number. Arrows indicate sub-G1 cells (apoptotic). Flow cytometric determination of cell cycle distribution of LNC cells following 24 hr (A-C) or 42 hr (D-F) of treatment: Control (A) and (D), scrambled IL-10 dsScr (B) and (E), RNAi IL-10 (RNAi) (C) and (F). The distribution of cells in each phase of the cell cycle following treatment was summed to give the percentage of cycling cells. The percentage of apoptotic cells is expressed as a percentage of the whole gated population.

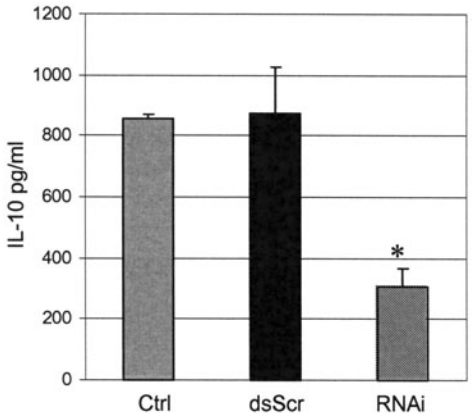

Figure 5. IL-10 protein analysis by ELISA. The amount of IL-10 protein in LNC supernatants was measured by ELISA. Columns correspond to groups treated for 72 hr with either 2 µM IL-10 RNAi (hatched bar), 2 µM dsScr (black bar), or untreated control (gray bar). Error bars are the SEM of triplicate results. Asterisks indicate $P < 0.05$ for a Student's *t*-test comparing dsScr to RNAi.

IL-10 RNAi decreases IL-10 message as analysed by real-time RT-PCR

Real-time RT-PCR was employed to determine the amount of IL-10 message at 72 hr (Figure 6). Real-time PCR was performed with the Taqman™ assay, and the amount of RNA message was normalized with ribosomal 18S. The differences in the cycle threshold (CT) values between ribosomal 18S and IL-10 gene expression (Delta CT) were calculated, and a comparison value between control and 2 µM RNAi-treated LNC cells was determined (Delta Delta CT). The Delta Delta CT value was found to be 1.12 ± 0.30. A higher CT value for RNAi indicates less RNA, as more cycles were required to reach the same RNA density point on the graph.

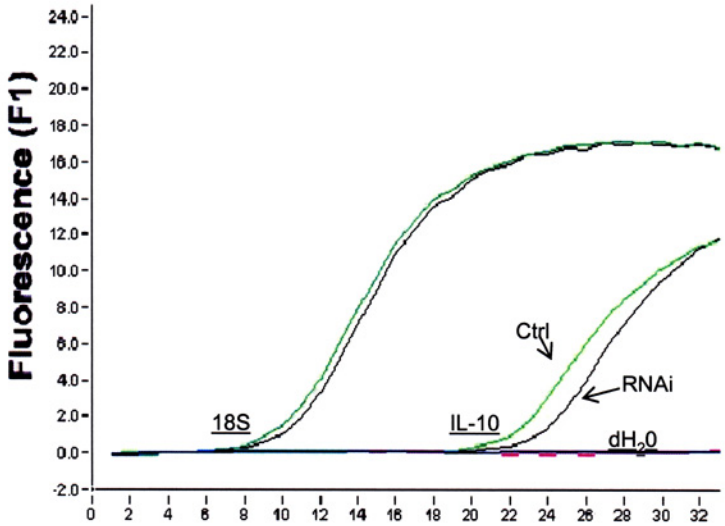

Figure 6. IL-10 message analysis by real-time RT-PCR. Fluorescence of Taqman™ reporter dyes for IL-10 and ribosomal 18S are labeled. Black curves represent results from LNC cells treated for 72 hr with 2 µM IL-10 RNAi. Gray curves are untreated control. Ribosomal 18S was used to normalize samples. The graph is representative of three real-time PCR reactions.

Analysis of selected genes by RT-PCR

Using 2 µM RNAi, a dose 10 times smaller than that of antisense, there is a decrease in IL-10, cdc25C, IL-10 R1, and p27 expression at 48 hr. In contrast, no change was observed for IL-10 R2. *IL-10* homologs were also analyzed after 48 hr of RNAi treatment, but no significant difference was observed for IL-19, IL-22, or IFN-lambda (data not shown). The mRNA levels of TNF-alpha, while not significantly affected, were increased to 114.4% of control (Figure 7A). At a dose of 1.5 µM RNAi, TNF-alpha levels also increased to 128% of control after 48 hr (data not shown). The dsScr sequence, which was used as a negative control for nonspecific effects, did not have any significant effects. The samples of gel electrophoresis of PCR amplicons shown (Figure 7B) are representative of triplicate gels. The mRNA expression of apoptotic regulators was analyzed to determine possible pathways influenced by IL-10 RNAi (Figure 8A). There was a significant reduction in the RNA message for the prosurvival protein Bcl7C ($P = 0.027$), and an increase in the levels of the proapoptotic Bax. Bcl2 levels were not significantly affected. The ratio of prosurvival Bcl2 to proapoptotic Bax was reduced by 37.4% (± 5.7%) after treatment. The gel samples shown are representative of triplicate gels (Figure 8B).

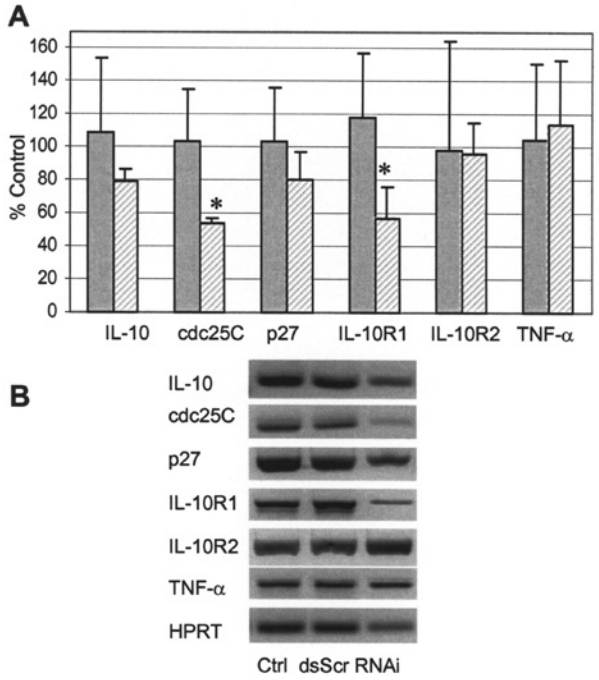

Figure 7. Semiquantitative RT-PCR analysis of IL-10 and critical cell cycle components. (A) Graphic analysis of semiquantitative RT-PCR for IL-10, cdc25C, p27, IL-10 R1, IL-10 R2 and TNF-alpha RNA levels after 48 hours of treatment with either 2 µM IL-10 RNAi (hatched bars), 2 µM dsSCR (gray bars) as compared to an untreated control. Numbers correspond to the percentage of control values from triplicate gels and error bars to the SEM. Asterisks indicate $P < 0.05$ for a Student's *t*-test comparing dsScr to RNAi. (B) Representative PCR gels stained with ethidium bromide: Control (lane 1), 2 µM dsSCR (lane 2) and 2 µM IL-10 RNAi (lane 3).

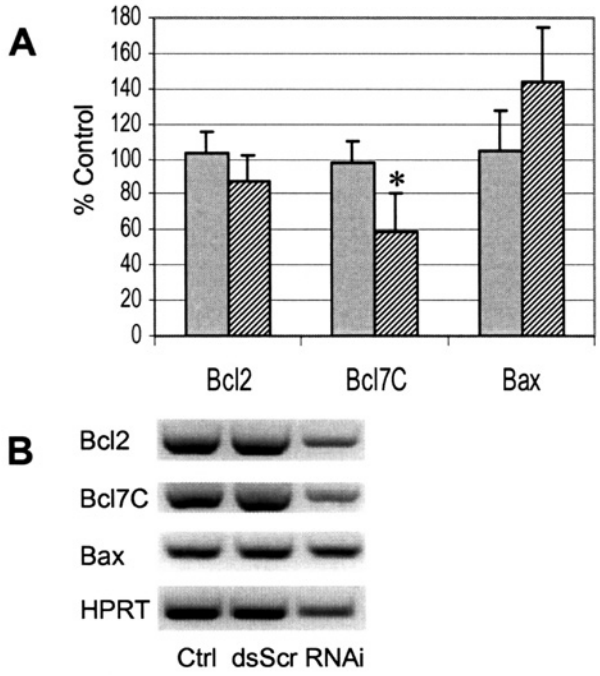

Figure 8. Semiquantitative RT-PCR analysis of apoptosis regulators. (A) Graphic analysis of semiquantitative RT-PCR for Bcl2, Bcl7C, and Bax RNA levels after 48 hr of treatment with either 2 µM IL-10 RNAi (hatched bars) or 2 µM dsScr (gray bars) when compared to an untreated control. Numbers represent percent of control values from triplicate gels. Error bars are SEM. Asterisks indicate $P < 0.05$ for a Students *t*-test comparing dsScr to RNAi. (B) Representative PCR gels stained with ethidium bromide. Lane 1 is control, lane 2 is 2 µM dsScr and lane 3 is 2 µM IL-10 RNAi.

Discussion

RNAi was used to decrease IL-10 levels and employed interference with 21 nucleotide dsRNA oligos termed short-interfering RNAi (siRNAi). The targeted RNA sequences, unique for IL-10, appear in the idealized model of RNA tertiary structure on the open stretch of a hairpin. The structure and folding of the RNAi are known to be important (34). IL-10 had previously been shown to be critical to LNC malignancy and was an ideal target candidate for this B-1 type cell. Here *IL-10* RNA interference was used to reduce the levels of *IL-10* mRNA and to significantly decrease the translation into IL-10 protein, as measured by ELISA. Both PCR and real-time Taqman™ assays demonstrated a sustained decrease in *IL-10* mRNA levels following RNAi treatment. RNA interference of IL-10 subsequently induced the apoptosis of these malignant cells.

Although listed by the Cancer Genome Anatomy Project of the National Cancer Institute (45) as antiapoptotic, the role of IL-10 in leukemia has been controversial. Once characterized as apoptotic (1), its role as a growth factor has recently attracted interest, with one lab calling IL-10 "the most relevant cytokine for B cell survival both in mice and humans", with important growth factor effects (46). IL-10 may be responsible for the long-lived, self-renewing aspects of B-1 cells. IL-10 has been found to be antiapoptotic, but the mechanism by which it functions as an antiapoptotic agent is not clear. IL-10 is well known to signal through the Jak/Stat pathway. It induces the tyrosine phosphorylation of tyk2 and Jak1, and signals through STAT1 and STAT3 (47). STAT 3 has been implicated in the prevention of apoptosis (48, 49) and is differentially expressed in normal, self-renewing B-1 cells as compared to conventional B lymphocytes (50).

In addition, IL-10 might influence the apoptotic pathway by the regulation of the *Bcl* family (47, 51). The balance between the antiapoptotic Bcl2 and the proapoptotic Bax is an important clinical parameter in CLL. In our studies, the ratio of Bcl2/Bax was reduced by 37.4% after RNAi treatment, which is consistent with the induction of apoptosis and supportive of a role for IL-10 in this pathway. This is consistent with our previous studies, in which NZB *IL-10* knockout B cells demonstrated a decrease in Bcl2 family expression relative to IL-10-producing NZB (9). The levels of apoptotic proteins may help us to identify patients who might benefit from blocking IL-10, or IL-10 inducible genes, in a clinical setting. We also found that IL-10 RNAi reduced the expression of Bcl7C. That the expression of the *Bcl7C* gene (52) was reduced by IL-10 RNAi suggests that IL-10 may influence other members of the *Bcl* family besides the well-known *Bcl2*.

Cell cycle perturbations are a hallmark of B-cell malignancies. Published reports have shown $p27^{Kip1}$ to be involved in CLL (53), and an elevated $p27^{Kip1}$ status was linked with antiapoptosis. Also, $p27^{Kip1}$ is an adverse prognostic factor in B-CLL, and its expression was linked to the defect in apoptosis (54). Our earlier gel shift assays showed that antisense IL-10 treatment decreases STAT binding to a STAT-inducible element in the $p27^{Kip1}$ promoter, and that $p27^{Kip1}$ is down-regulated in antisense IL-10 treated cells, but not in control oligo treated cells (12). We now extend this analysis further, with IL-10 RNAi treatment of the NZB malignant B-1 line, LNC. RNAi, specific for IL-10, decreased $p27^{Kip1}$ levels as well.

Published microarray analysis suggested a role for cdc25C in the cell cycle regulation of CLL cells (55, 56). IL-10 RNAi treatment resulted in a decrease in the levels of *cdc25C* mRNA levels. IL-10 RNAi effectively reproduced the observed cell cycle changes induced by antisense IL-10 at a much lower concentration (12). Semiquantitative RT-PCR analysis shows *cdc25C* message was down-regulated ($P < 0.024$ compared to scrambled) when IL-10 was decreased by RNAi treatment as compared to both the scrambled and the untreated control groups.

IL-10 RNAi was found initially to induce a G2/M block followed by apoptosis. Similar results were obtained by antisense IL-10 (12). One of the target genes profoundly affected by decreased IL-10 levels was *cdc25C*. This cell division control protein was initially called the M-phase inducer phosphatase; it is a dual specificity phosphatase that acts at the end of G2, controlling the entry of vertebrate cells into mitosis (57).

Bioinformatics has already identified an autocrine signaling loop for IL-10 and its receptor 1 (58). Our RT-PCR analysis of RNAi treatment showed that IL-10 R1 was markedly reduced by 12 hr and significantly reduced by 48 hr ($P = 0.035$), whereas IL-10 R2 was unchanged at 12 hr and remained slightly increased at 24 hr (data not shown) and 48 hr. This may indicate an autocrine feedback signal, which explains why cdc25C was decreased more than IL-10 at 48 hr. A less likely explanation, given the rapid onset of apoptosis, is that this RNAi sequence is relatively inefficient, and other areas of the gene might create a more dramatic decrease in IL-10 RNA levels.

RNAi shows great promise in the clinical setting (59). RNAi targeting of the Fas protein abrogated hepatocyte necrosis and inflammatory infiltrate (60). D-RNAi or a hybrid of messenger RNA-antisense DNA interference targeting *gag*/*pol* expression blocked viral gene replication completely (61). Here, IL-10 RNAi was shown to potently inhibit the growth of malignant B cells.

IL-10 is known to regulate the response of inflammatory cytokines such as TNF-alpha. IFN-gamma was not detectable in LNC by RT-PCR before or after RNAi treatment (data not shown). Chronic intestinal inflammation in IL-10-deficient mice has been shown to involve TNF. IL-10 exerts a direct effect on the 3' AU-rich elements of TNF mRNA to inhibit the mRNA's translation, and the balance between TNF and IL-10 is thought to be critical (62). We examined TNF-alpha by RT-PCR and found that RNAi treatment increased TNF-alpha levels, but not

significantly. However, increased TNF and decreased IL-10 levels lead to a shift in the balance of TNF-alpha/IL-10 and may be partly responsible for the apoptosis seen after IL-10 RNAi treatment. Autocrine IL-10 may have a subtle influence on several pathways simultaneously, not exclusively by receptor-mediated events.

The efficiency of this RNAi sequence is typical for those reported to be modeled according to Tuschl rules (63). In this system, there were dramatic effects on cell survival and on IL-10 protein levels through RNAi, although the decrease in *IL-10* RNA was less dramatic. Autocrine signaling may be responsible for this effect. In a murine model of tuberculosis, a 23% reduction in IL-10 protein was attributed to the induction of type 1 cytokines (64).

Clarifying IL-10's role in biology is an area of intensive, ongoing research. Blocking IL-10 may be of clinical value in cancer treatment. IL-10 can induce resistance to apoptosis, evasion of host defense, and increased resistance to chemotherapeutics. However, blocking IL-10 may have deleterious effects leading to inflammation, macrophage activation, and granuloma formation. IL-10's role in macrophage deactivation has been implicated in Crohn's disease. These negative factors involved with removing IL-10 might be overcome through dosage or localized delivery of the IL-10 blockade.

Based on the NZB mouse model, IL-10 is required for CD5+ B-1 cell malignancy. We have recently characterized an NZB *IL-10* knockout mouse strain with a dramatic decrease in the appearance of B-cell malignancy (65). In response to treatment with IL-10 RNAi, malignant B-1 cells had decreased levels of IL-10 protein as well as decreased *IL-10* and *cdc25C* RNA message. Cells underwent a G2/M cell cycle block and apoptosis. RNAi IL-10 treatment induced a significant decrease in cdc25C and IL-10 R1 as measured by RT-PCR. This paper demonstrates that IL-10 has a key role in the survival of malignant B-1 cells in the NZB model of CLL. These data suggest that blocking IL-10 or IL-10 inducible genes may be of potential value, either alone or in combination therapy, in treating certain leukemias.

Abbreviations

CLL, chronic lymphocytic leukemia; CT, cycle threshold; dsScr, scrambled dsRNA; RNAi, RNA interference

Acknowledgements

Our grateful appreciation to R. Donnely for technical assistance. This work was supported by grants from the National Institutes of Health and the New Jersey Commission on Cancer Research. This work is in partial fulfillment of the PhD thesis for Brian McCarthy, Department of Experimental Pathology and Laboratory Medicine, GSBS-UMDNJ.

References

1. Fluckiger A, Durand I, Banchereau J. IL-10 induces apoptotic cell death of B-chronic lymphocytic leukemia cells. *J Exp Med* 1994; **179**: 91-9. (PMID: 8270886)

2. Jurlander J, Chun-Fai L, Tan J, Chuan-Chu C, Geisler CH, Schriber J, Blumenson LE, Narula SK, Baumann H, Caligiuri MA. Characterization of interleukin-10 receptor expression on B-cell chronic lymphocytic leukemia cells. *Blood* 1997; **89**: 4146-52. (PMID: 9166857)

3. Morabito F, Filangeri M, Sculli G, Oliva B. *In vitro* modulation of bcl-2 protein expression, drug-induced apoptosis and cytotoxicity by interleukin-10 in chronic lymphocytic leukemia. *Haematologica* 1998; **83**: 1046-8. (PMID: 9864930)

4. Knauf WU, Ehlers B, Bisson S, Thiel E. Serum levels of interleukin-10 in B-cell chronic lymphocytic leukemia. *Blood* 1995; **88**: 4382-3. (PMID: 7492801)

5. Kamper EF, Papaphilis AD, Angelopoulou MK, Kopeikina LT, Siakantaris MP, Pangalis GA, Stavridis JC. Serum levels of tetranectin, intercellular adhesion molecule-1 and interleukin-10 in B-chronic lymphocytic leukemia. *Clin Biochem* 1999; **32**: 639-45. (PMID: 10638947)

6. Fayad L, Keating MJ, Reuben JM, O'Brien S, Lee BN, Lerner S, Kurzrock R. Interleukin-6 and interleukin-10 levels in chronic lymphocytic leukemia: correlation with phenotypic characteristics and outcome. *Blood* 2001; **97**: 256-63. (PMID: 11133769)

7. Peng B, Sherr DH, Mahboudi F, Hardin J, Sharer L, Raveche ES. A cultured malignant B-1 line serves as a model for Richter's syndrome. *J Immunol* 1994; **153**: 1869-80. (PMID: 8046247)

8. Phillips J, Mehta K, Fernandez C, Raveche ES. The NZB mouse as a model for CLL. *Cancer Res* 1992; **52**: 437-43. (PMID: 1370214)

9. Czarneski J, Lin Y, Chong S, McCarthy B, Parker G, Fernandes H, DeCotiis C, Huppi K, Marti G, Mansour A, Raveche ES. Studies in NZB IL-10 knockout mice of the requirement of IL-10 for progression of B cell lymphoma. *Leukemia* 2004; **18**: 597-606. (PMID: 14712288)

10. Parker G, Peng B, He M, Gould-Fogerite S, Chou C, Raveche ES. *In vivo* and *in vitro* antiproliferative effects of antisense IL-10 oligonucleotides. *Meth Enzymol* 1999; **314**: 411-29. (PMID: 10565029)

11. Ramachandra S, Metcalf R, Fredrickson T, Marti G, Raveche ES. Requirement for increased IL-10 in the development of B-1 lymphoproliferative disease in a murine model of CLL. *J Clin Invest* 1996; **98**: 1788-93. (PMID: 8878429)

12. Chong SY, Lin YC, Czarneski J, Zhang M, Coffman F, Kashanchi F, Raveche ES. Cell cycle effects of IL-10 on malignant B-1 cells. *Genes Immun* 2001; **2**: 239-47. (PMID: 11528515)

13. Guo S, Kemphues KJ. *Par-1*, a gene required for establishing polarity in C. elegans embryos, encodes a putative Ser/Thr kinase that is asymmetrically distributed. *Cell* 1995; **81**: 611-20. (PMID: 7758115)

14. Fire A, Xu S, Montgomery MK, Kostas SA, Driver SE, Mello CC. Potent and specific genetic interference by double-stranded RNA in *Caenorhabditis elegans*. *Nature* 1998; **391**: 806-11. (PMID: 9486653)

15. Napoli C, Lemieux C, Jorgensen RA. Introduction of a chalcone synthase gene into petunia results in reversible co-suppression of homologous genes in trans. *Plant Cell* 1990; **2**: 279-89. (PMID: 12354959)

16. Jorgensen RA, Cluster PD, English J, Que Q, Napoli CA. Chalcone synthase cosuppression phenotypes in petunia flowers: comparison of sense vs. antisense constructs and single-copy vs. complex T-DNA sequences. *Plant Mol Biol* 1996; **31**: 957-73. (PMID: 8843939)

17. Ingelbrecht I, Van Houdt H, Van Montagu M, Depicker A. Posttranscriptional silencing of reporter transgenes in tobacco correlates with DNA methylation. *Proc Natl Acad Sci U S A* 1994; **91**: 10502-6. (PMID: 7937983)

18. Cogoni C, Irelan JT, Schumache M, Schmidhauser T, Selker EU, Macino G. Transgene silencing of the *al-1* gene in vegetative cells of *Neurospora* is mediated by a cytoplasmic effector and does not depend on DNA-DNA interactions or DNA methylation. *EMBO J* 1996; **15**: 3153-63. (PMID: 8670816)

19. Shi Y. Mammalian RNAi for the masses. *Trends Genet* 2003; **19**: 9-12. (PMID: 12493242)

20. Hannon GJ. RNA interference. *Nature* 2002; **418**: 244-51. (PMID: 12110901)

21. McManus MT, Sharp PA. Gene silencing in mammals by small interfering RNAs [review]. *Nat Rev Genet* 2002; **3**: 737-47. (PMID: 12360232)

22. Guru T. A silence that speaks volumes. *Nature* 2000; **404**: 804-8. (PMID: 10786767)

23. Cogoni C, Macino G. Post-transcriptional gene silencing across kingdoms. *Curr Opin Genet Dev* 2000; **10**: 638-43. (PMID: 11088014)

24. Kennerdell JR, Carthew RW. Heritable gene silencing in *Drosophila* using double-stranded RNA. *Nat Biotechnol* 2000; **18**: 896-8. (PMID: 10932163)

25. Lum L, Yao S, Mozer B, Rovescalli A, Von Kessler D, Nirenberg M, Beachy PA. Identification of hedgehog pathway components by RNAi in *Drosophila* cultured cells. *Science* 2003; **299**: 2039-45. (PMID: 12663920)

26. Sui G, Soohoo C, Affar EB, Gay F, Shi Y, Forrester WC, Shi Y. A DNA vector-based RNAi technology to suppress gene expression in mammalian cells. *Proc Natl Acad Sci U S A* 2002; **99**: 5515-20. (PMID: 11960009)

27. Elbashir SM, Harborth J, Lendeckel W, Yalcin A, Weber K, Tuschl T. Duplexes of 21-nucleotide RNAs mediate RNA interference in cultured mammalian cells. *Nature* 2001; **411**: 494-8. (PMID: 11373684)

28. Paddison PJ, Caudy A, Hannon GJ. Stable suppression of gene expression by RNAi in mammalian cells. *Proc Natl Acad Sci U S A* 2002; **99**: 1443-8. (PMID: 11818553)

29. Paul CP, Good PD, Winer I, Engelke DR. Effective expression of small interfering RNA in human cells. *Nat Biotechnol* 2002; **20**: 505-8. (PMID: 11981566)

30. Brummelkamp TR, Bernards R, Agami R. A system for stable expression of short interfering RNAs in mammalian cells. *Science* 2002; **296**: 550-3. (PMID: 11910072)

31. Zuker M, Stiegler P. Optimal computer folding of large RNA sequences using thermodynamic and auxiliary information. *Nucleic Acids Res* 1981; **9**: 133-48. (PMID: 6163133)

32. Hofacker IL, Fontana W, Stadler PF, Bonhoeffer S, Tacker M, Schuster P. Fast folding and comparison of RNA secondary structures. *Monatsh Chem* 1994; **125**: 167-188.

33. McCaskill JS. The equilibrium partition function and base pair binding probabilities for RNA secondary structures. *Biopolymers* 1990; **29**: 1105-19. (PMID: 1695107)

34. Kretschmer-Kazemi Far R, Sczakiel G. The activity of siRNA in mammalian cells is related to structural target accessibility: a comparison with antisense oligonucleotides. *Nucleic Acids Res* 2003; **31**: 4417-24. (PMID: 12888501)

35. Tabara H, Grishok A, Mello CC. RNAi in C. elegans: soaking in the genome sequence. *Science* 1998; **282**: 430-1. (PMID: 9841401)

36. Fiorentino DF, Bond MW, Mosmann TR. Two types of mouse T helper cell. IV. Th2 clones secrete a factor that inhibits cytokine production by Th1 clones. *J Exp Med* 1989; **170**: 2081-95. (PMID: 2531194)

37. Rennick D, Fort MM, Davidson NJ. Studies with IL-10 mice: an overview. *J Leukoc Biol* 1997; **61**: 389-96. (PMID: 9103224)

38. Lalani I, Bhol K, Ahmed AR. Interleukin-10: biology, role in inflammation and autoimmunity. *Ann Allergy Asthma Immunol* 1997; **79**: 469-83. (PMID: 9433360)

39. Mullins DW, Martins RS, Burger CJ, Elgert KD. Tumor cell-derived TGF- and IL-10 dysregulate paclitaxel-induced macrophage activation. *J Leukoc Biol* 2001; **69**: 129-37. (PMID: 11200057)

40. Malefyt R. Interleukin 10. London: Academic Press; 1998.

41. O'Garra A, Chang R, Go N, Hastings R, Haughton G, Howard M. Ly-l B (B-1) cells are the main source of B-cell-derived interleukin-10. *Eur J lmmunol* 1992; **22**: 711-7. (PMID: 1547817)

42. De Vita F, Orditura M, Galizia G, Romano C, Infusino S, Auriemma A, Lieto E, Catalano G. Serum interleukin-10 levels in patients with advanced gastrointestinal malignancies. *Cancer* 1999; **86**: 1936-43. (PMID: 10570416)

43. Alizadeh AA, Eisen MB, Davis RE, Ma C, Lossos IS, Rosenwald A, Boldrick JC, Sabet H, Tran T, Yu X, Powell JI, Yang L, Marti GE, Moore T, Hudson J Jr, Lu L, Lewis DB, Tibshirani R, Sherlock G, Chan WC, Greiner TC, Weisenburger DD, Armitage JO, Warnke R, Levy R, Wilson W, Grever MR, Byrd JC, Botstein D, Brown PO, Staudt LM. Distinct types of diffuse large B-cell lymphoma identified by gene expression profiling. *Nature* 2000; **403**: 503-11. (PMID: 10676951)

44. Alas S, Emmanouilides C, Bonavida B. Inhibition of interleukin 10 by rituximab results in down-regulation of bcl-2 and sensitization of B-cell non-Hodgkin's lymphoma to apoptosis. *Clin Cancer Res* 2001; **7**: 709-23. (PMID: 11297268)

45. National Cancer Institute CGAP Gene Ontology browser. URL: http://cgap.nci.nih.gov/Genes/GOBrowser

46. Gary-Gouy H, Harriague J, Bismuth G, Platzer C, Schmitt C, Dalloul AH. Human CD5 promotes B-cell survival through stimulation of autocrine IL-10 production. *Blood* 2002; **100**: 4537-43. (PMID: 12393419)

47. Finbloom DS, Winestock KD. IL-10 induces the tyrosine phosphorylation of tyk2 and Jak1 and the differential assembly of STAT1 alpha and STAT3 complexes in human T cells and monocytes. *J Immunol* 1995; **155**: 1079-90. (PMID: 7543512)

48. Alas S, Bonavida B. Inhibition of constitutive STAT3 activity sensitizes resistant non-Hodgkin's lymphoma and multiple myeloma to chemotherapeutic drug-mediated apoptosis. *Clin Cancer Res* 2003; **9**: 316-26. (PMID: 12538484)

49. Fukada T, Hibi M, Yamanaka Y, Takahashi-Tezuka M, Fuji-tani Y, Yamaguchi T, Nakajima K, Hirano T. Two signals are necessary for cell proliferation induced by a cytokine receptor gp130: involvement of STAT3 in anti-apoptosis. *Immunity* 1996; **5**: 449-60. (PMID: 8934572)

50. Karras JG, Wang Z, Huo L, Howard RG, Frank DA, Rothstein TL. Signal transducer and activator of transcription-3 (STAT3) is constitutively activated in normal, self-renewing B-1 cells but only inducibly expressed in conventional B lymphocytes. *J Exp Med* 1997; **185**: 1035-42. (PMID: 9091577)

51. Morabito F, Filangeri M, Callea I, Sculli G, Callea V, Fracchiolla NS, Neri A, Brugiatelli M. Bcl-2 protein expression and p53 gene mutation in chronic lymphocytic leukemia: correlation with the *in vitro* sensitivity to chlorambucil and purine analogs. *Haematologica* 1997; **82**: 16-20. (PMID: 9107076)

52. Jadayel D, Osborne LR, Zani VJ, Coignet LFA, Tsui LC, Scherer SW, Dyer MJS. The BCL7 gene family: deletion of the BCL7B gene in Williams syndrome. *Gene* 1998; **224**: 35-44. (PMID: 9931421)

53. Vrhovac R, Delmer A, Tang R, Marie JP, Zittoun R, Ajchenbaum-Cymbalista F. Prognostic significance of the cell cycle inhibitor p27Kip1 in chronic B-cell lymphocytic leukemia. *Blood* 1998; **91**: 4694-700. (PMID: 9616167)

54. Magnac C, Porcher R, Davi F, Nataf J, Payelle-Brogard B, Tang RP, Oppezzo P, Levy V, Digheiro G, Ajchenbaum-Cymbalista F. Predictive value of serum thymidine kinase level for Ig-V mutational status in B-CLL. *Leukemia* 2003; **17**: 133-7. (PMID: 12529670)

55. Klein U, Tu Y, Stolovitsky GA, Mattioli M, Cattoretti G, Husson H, Freedman A, Inghirami G, Cro L, Baldini L, Neri A, Califano A, Dalla-Tavera R. Gene expression profiling of B cell chronic lymphocytic leukemia reveals a homogeneous phenotype related to memory B cells. *J Exp Med* 2001; **194**: 1625-38. (PMID: 11733577)

56. Jelinek DF, Tschumper RC, Stolovitzky GA, Iturria SJ, Tu Y, Lepre J, Shah N, Kay NE. Identification of a global gene expression signature of B-chronic lymphocytic leukemia. *Mol Cancer Res* 2003; **1**: 346-61. (PMID: 12651908)

57. Krek W, Nigg E. Mutations of p34cdc2 phosphorylation sites induce premature mitotic events in HeLa cells: evidence for a double block to p34cdc2 kinase activation in vertebrates. *EMBO J* 1991; **10**: 3331-41. (PMID: 1655418)

58. Graeber TG, Eisenberg D. Bioinformatic identification of potential autocrine signaling loops in cancers from gene expression profiles. *Nat Genet* 2001; **29**: 295-300. (PMID: 11685206)

59. Lieberman J, Song E, Lee SK, Shankar P. Interfering with disease: opportunities and roadblocks to harnessing RNA interference. *Trends Mol Med* 2003; **9**: 397-403. (PMID: 13129706)

60. Song E, Lee SK, Wang J, Ince N, Ouyang N, Min J, Chen J, Shankar P, Lieberman J. RNA interference targeting Fas protects mice from fulminant hepatitis. *Nat Med* 2003; **9**: 347-51. (PMID: 12579197)

61. Lin SL, Ying SY. D-RNAi (messenger RNA-antisense DNA interference) as a novel defense system against cancer and viral infections. *Curr Cancer Drug Targets* 2001; **1**: 241-7. (PMID: 12188882)

62. Kontoyiannis D, Kotlyarov A, Carballo E, Alexopoulou L, Blackshear PJ, Gaestel M, Davis R, Flavell R, Kollias G. Interleukin-10 targets p38 MAPK to modulate ARE-dependent TNF mRNA translation and limit intestinal pathology. *EMBO J* 2001; **20**: 3760-70. (PMID: 11447117)

63. Boese QF, Scaringe SA, Marshall WS. siRNA as a tool for streamlining functional genomic studies. *Targets* 2003; **2**: 93.

64. Leemans JC, Juffermans NP, Florquin S, van Rooijen N, Vervoordeldonk MJ, Verbon A, van Deventer SJH, van der Poll T. Depletion of alveolar macrophages exerts protective effects in pulmonary tuberculosis in mice. *J Immunol* 2001; **166**: 4604-11. (PMID: 11254718)

65. Czarneski J, Lin YC, Chong S, McCarthy B, Fernandes H, Parker G, Mansour A, Huppi K, Marti GE, Raveche E. Studies in NZB IL-10 knockout mice of the requirement of IL-10 for progression of B-cell lymphoma. *Leukemia* 2004; **18**: 597-606. (PMID: 14712288)

66. National Center for Biotechnology Information web site. URL: http://www.ncbi.nlm.nih.gov/

67. The Zuker Group: Algorithms, thermodynamics and databases for RNA secondary structure. URL: http://www.bioinfo.rpi.edu/~zukerm/rna/

68. Tuschl T, Zamore PD, Lehmann R, Bartel DP, Sharp PA. Targeted mRNA degradation by double-stranded RNA *in vitro*. *Genes Dev* 1999; **13**: 3191-7. (PMID: 10617568)

69. Mosmann T. Rapid colorimetric assay for cellular growth and survival: application to proliferation and cytotoxicity assays. *J Immunol Methods* 1983; **65**: 55-63. (PMID: 6606682)

70. Nicoletti I, Migliorati G, Pagliacci MC, Grignani F, Riccardi C. A rapid and simple method for measuring thymocyte apoptosis by propidium iodide staining and flow cytometry. *J Immunol Methods* 1991; **139**: 271-9. (PMID: 1710634)

Materials and methods

Cell line

LNC cells, an *in vitro* established line obtained from the lymph node of 1-yr-old NZB mice with CLL (7), were used as a source of malignant B-1 cells. Cells were maintained in Iscove's modified Dulbecco's medium supplemented with 10% fetal calf serum, 200 mM L-glutamine, and a 1% solution of penicillin, streptomycin, and fungizone (Gibco BRL, Rockville, MD). All experiments were performed with an initial cell viability of greater than 90%. Cells were counted using an automated counter (Coulter, Miami, FL) according to the manufacturer's instructions.

RNA modeling

Sequences obtained from the NCBI web site (66) were entered into Mfold Software (D. Stewart and M. Zuker, Washington University) (67) to model the optimal area of the IL-10 mRNA for RNAi targeting (31, 32, 33).

Synthesis of dsRNAi

RNA inhibitory and corresponding scrambled sequences were synthesized by *in vitro* transcription at the University of Medicine and Dentistry of New Jersey (UMDNJ) Molecular Resource Facility as previously described (68). Briefly, the 21-nucleotide murine IL-10 RNAi sense strand (5' GCCUUAUCGGAAAUGAUCCdTdT 3') starts at nucleotide 319 on the *IL-10* mRNA (GenBank Accession No. M37897) and ends with a single T-for-A substitution at nucleotide 338 to complete the final TT overhang motif. The RNAi antisense strand (5' GGAUCAUUUCCGAUAAGGCdTdT 3'), scrambled sense (5' CUGUCAGAAGGCUAUCUCAdTdT 3'), and scrambled antisense (5' UGAGAUAGCCUUCUGACAGdTdT 3') were synthesized with 2 deoxy thymidines (dT) as the final bases. Neither the IL-10 nor IL-10 scrambled sequences match any known murine gene in the NCBI sequence database. Paired single-stranded sequences, RNAi and scrambled, were diluted in DEPC water, annealed in 20% annealing buffer, 100 mM potassium acetate (EMScience, Gibbstown, NJ), 30 mM Hepes-KOH at pH 7.4, 2 mM magnesium acetate (JT Baker, Phillipsburg, NJ) for 1 min at 90°C, followed by incubation for 1 hr at 37°C, added to Iscove's Modified Dulbecco's medium, and used at a final concentration of between 0.2-2 µM.

Cell proliferation study

Treated or untreated LNC cells (5×10^4) in 100 µl of complete media with or without oligonucleotide were plated in triplicate wells in 96-well flat-bottomed plates. Twenty microliters of 3-(4,5-Dimethyl-thiazol-2-yl)-2,5-diphenyl-tetrazolium bromide (Sigma) (5 mg/ml MTT in PBS) were added to each well and incubated in a 37°C incubator with 5% CO_2 for 3-4 hr. The plates were then processed as described previously (69).

Flow cytometry

Flow cytometry was used to detect cell cycle changes and apoptosis by staining the DNA with PI (Calbiochem, San Diego, CA). For PI staining, 1×10^6 cells were stained with hypotonic PI (0.05 mg/ml PI, 0.1% Triton X-100). FACS data were acquired on a Becton Dickinson FACS® caliber with a 488-nm argon laser. Acquisition was carried out using CELLQuest software (Becton Dickinson, San Jose, CA) and analysis was performed using ModFit LT software (Verity House, Inc., Topsham, ME) as previously described (70). Apoptotic cells were calculated from the $subG_1$ fraction.

ELISA

The levels of IL-10 in the supernatants were determined using a commercially available IL-10 immunoassay (Biosource, Camarillo, CA). Supernatants were spun at 1000 rpm for 5 min to pellet the cells and were then transferred to a new tube. Supernatants were used undiluted and compared to a standard curve. A monoclonal antimouse IL-10 antibody was precoated on 96-well plates and developed with peroxidase according to the Biosource protocol. This ELISA is sensitive to 20 pg/ml IL-10.

RT-PCR

RNA isolation for transcriptional determinations by RT-PCR were carried out using RNeasy mini-kit (Qiagen, Valencia, CA). Complementary DNA production was performed with Amplitaq Gold (Roche, Indianapolis, IN). The primers, defined after a BLAST search, were obtained from Operon (Alameda, CA) or the University of Medicine and Dentistry of New Jersey (UMDNJ) Molecular Resource Facility and are listed along with the GenInfo Identifier (GI) number, and the product size and nucleotide span in Table 1.

Following the PCR reaction, the amplicons were electrophoresed, stained with ethidium bromide, and analyzed with a fluorimager (Molecular Dynamics, Sunnyvale, CA). The ratio of the gene of interest compared to the housekeeping gene hypoxanthine phosphoribosyltransferase (*HPRT*) was obtained by using the sum above background method, as recommended by the manufacturer. Significance was determined by Student's *t*-test using the standard deviation from the mean.

Real-time RT-PCR

RNA was isolated as previously described. Quantitative real-time RT-PCR was performed with the Light Cycler version 2 (Roche, Indianapolis, IN) using commercially available Taqman™ (PE Biosystems, Foster City, CA) primers for IL-10 and ribosomal 18S. Equal amounts of each of the RNA samples, quantified using ribosomal 18S as a standard, were reverse transcribed and used as PCR templates to obtain the CT value. The IL-10 CT value was normalized with respect to the CT value for ribosomal 18S to obtain Delta CT. The difference between treatment and control was calculated to obtain the change in Delta CT (Delta Delta CT) representing the real increase in expression.

Table 1. Genes, PCR primers and products.

Gene		PCR Primer Sequences	PCR Product	
Name	GI No.		Size (bp)	Nucleotides Spanned
IL-10	6754317	5': CGGGAAGACAATAACTG	186	148-333
		3': CATTTCCGATAAGGCTTGG		
IFN-γ	28501526	5': AACGCTACACACTGCATCTTG	237	112-348
		3': GACTTCAAAGAGTCTGAGG		
TNF-α	7305584	5': AGTGGTGCCAGCCGATGGGTTGT	253	537-789
		3': GCTGAGTTGGTCCCCCTTCTCCAG		
Bax	17390521	5': CCAAGAAGCTGAGCGAGTGTCTC	146	235-381
		3': AGTTGCCATCAGCAAACATGTCA		
Bcl2	6753167	5': CAGCTGCACCTGACG	303	343-641
		3': AGAGACAGCCAGGAG		
Bcl7C	13542972	5': GGCGACCATCGAGAAGGTCCG	318	305-622
		3': GTTGGTGATCCAGGGCGGC		
cdc25C	13435584	5': CACCAGTTTAAAGGCATTGG	230	519-748
		3': GACTTAAGCCCTTGGCGTCC		
IL-10R1	6680388	5': CTGAGCCTAGAATTCATTGCATAC	388	122-509
		3': CATAGATGATGCCGTCCATTGCTT		
IL-10R2	17646387	5': CCACCCCCTGAGAAGGTC	599	80-678
		3': CAGGAAGGGGTTATTTCG		
p27	17939614	5': GGCTCTGCTCCATTTGACTG	393	342-734
		3': CCTGCCATTCGTATCTGCCC		
IL-19	28482156	5': CCGGATCCCTCAGTTCATATCTACAGTCTTAG	477	166-643
		3': TTGAATTCAGGCTGCAGGAGTTTCCAGATG		
IL-22	8393604	5': AAATGCGCTGCCCGTCAACAC	192	146-337
		3': ACCTGCTTCATCAGGTAGCAC		
IFN-λ	27261790	5': GCGGTACCATGACTGGGGACTGCACGCCAGTG	595	9-603
		3': CGGAATTCAGGTGGACTCAGGGTGGGTTGA		
HPRT	13435620	5': GTTGGATACAGGCCAGACTTTGTTG	162	575-737
		3': GATTCAACTTGCGCTCATCTTAGGC		

Contact

Address correspondence to:

Elizabeth Raveche
UMDNJ MSC C512
185 South Orange Ave
Newark, NJ 07103
USA
Tel.: + 1 973 972 5240
Fax: + 1 973 972 7293
E-mail: raveches@umdnj.edu